Heterozygous mutations of the integrin αIIbR995/β3D723 intracytoplasmic salt bridge cause macrothrombocytopenia, platelet functional defects and enlarged α-granules

Marie Favier, Jean-Claude Bordet, Rémi Favier, Vasiliki Gkalea, Xavier Pillois, Philippe Rameau, Najet Debili, Marie-Christine Alessi, Paquita Nurden, Hana Raslova, et al.

Heterozygous mutations of the integrin αIIbR995/β3D723 intracytoplasmic salt bridge cause macrothrombocytopenia, platelet functional defects and enlarged α-granules

Favier M PD[1,2], Bordet JC PhD[3], Favier R MD[2,4], Gkalea V MD[4], Pillois X PhD[5], Rameau P PhD[7], Debili N PhD[2], Alessi MC MD[1] Nurden P MD[6], Raslova H PhD[2], and Nurden AT PhD[6]

[1]Laboratoire NORT, INSERM UMR 1062, INRA 1260, Université Aix Marseille, Marseille ; [2]INSERM UMR 1170, Gustave Roussy Cancer Campus, Université Pris-Saclay, Villejuif 94805, France; [3]Laboratoire d'Hémostase, Hôpital Edouard Herriot, Lyon et Laboratoire de Recherche sur l'Hémophilie, Faculté de Médecine Lyon-Est, Université Claude Bernard Lyon 1, Lyon, France ; [4]Assistance Publique -Hôpitaux de Paris, Hôpital A Trousseau, 75012 Paris, France; [5]Université de Bordeaux, INSERM U1034, Pessac, France; [6]Institut Hospitalo-Universitaire de Rythmologie et de Modélisation Cardiaque, Plateforme Technologique d'Innovation Biomédicale, Hôpital Xavier Arnozan, Pessac, France ; 7-PFIC, UMS AMMICA (UMS 3655 CNRS/US23 INSERM) , Gustave Roussy Cancer Campus , Villejuif 94805, France.

Short title: αIIbR995/β3D723 macrothrombocytopenia with large α-granules

Abstract word count: 188
Text word count: 4280
Figure number:4
Table number:1

Key words: inherited macrothrombocytopenia, integrin a2IIbb3, platelet function defects, enlarged a -granules

Correspondence : Remi Favier, Armand Trousseau children hospital, CRPP, Paris 75012, France. Phone: 33 01 44 73 69 49; Fax 33 01 44 73 63 33; e-mail: remi.favier@aphp.fr

ABSTRACT

Rare gain-of-function mutations within the *ITGA2B* or *ITGB3* genes have been recognized to cause macrothrombocytopenia (MTP). Here we report three new families with autosomal dominant (AD) MTP, two harboring the same mutation of *ITGA2B,* αIIb R995W, and a third family with an *ITGB3* mutation, β3D723H. The two mutated amino-acids are directly involved in the salt bridge linking the intra-cytoplasmic part of αIIb to β3 of the integrin αIIbβ3.

For all affected patients, the bleeding syndrome and MTP was mild to moderate. Platelet aggregation tended to be reduced but not absent. Electron microscopy associated with a morphometric analysis revealed large round platelets; a feature being the presence of abnormal large α-granules with some giant forms showing signs of fusion. Analysis of the maturation and development of megakaryocytes reveal no defect in their early maturation but abnormal proplatelet formation was observed with increased size of the tips.

Interestingly, this study revealed that in addition to the classical phenotype of patients with αIIbβ3 intracytoplasmic mutations, an abnormal maturation of α-granules. It will be interesting to determine if this feature is a characteristic of mutations disturbing the αIIb R995/β3 D723 salt bridge.

INTRODUCTION

Integrin αIIbβ3 is the platelet receptor for fibrinogen (Fg) and other adhesive proteins and mediates platelet aggregation playing a key role in hemostasis and thrombosis. It circulates on platelets in a low-affinity state becoming ligand-competent as a result of conformational changes induced by "inside-out" signaling following platelet activation (1). Inherited defects of αIIbβ3 with loss of expression and/or function are causal of Glanzmann thrombasthenia (GT), an autosomal recessive bleeding disorder (2,3). Rare gain-of-function mutations of the *ITGA2B* or *ITGB3* genes encoding αIIbβ3 also cause macrothrombocytopenia (MTP) with a low platelet count and platelets of increased size (3,4). Mostly heterozygous with autosomal dominant (AD) expression these include D621_E660del*, L718P, L718del and D723H mutations in β3, and G991C, G993del, R995Q or W in αIIb (Table I) (5-12). While Asp621_Glu660del affects the extracellular cysteine-rich βA domain of β3, the others affect transmembrane or intracellular cytoplasmic domains and in particular the salt bridge linking the negatively charged D723 of β3 with the positively charged R995 of the much studied GFFKR sequence of αIIb (13-15). These mutations permit residual or even total αIIbβ3 expression but give rise to conformation changes that propagate through the integrin and which are recognized by binding of the monoclonal antibody, PAC-1 (16). The MTP appears related to cytoskeletal changes during the late stages of megakaryocyte (MK) development and altered proplatelet formation (17-19). Yet, while most of the above variants combine MTP with a substantial loss of platelet aggregation and a GT-like phenotype, the D723H β3 substitution had no effect on platelet aggregation and was called a non-synonymous single nucleotide polymorphism (SNP) by the authors (6). This was surprising as another cytoplasmic domain mutation involving a near-neighbour Arg724Ter truncating mutation in β3, while not preventing αIIbβ3 expression gave a full GT phenotype (20). We recently reported a heterozygous intracytoplasmic β3 Leu718del that resulted in loss of synchronization between the cytoplasmic tails of β3 and αIIb; changes that gave moderate MTP, a reduced platelet aggregation response and, unexpectedly, enlarged α-granules (12). It

is in this context that we now report our studies on a second European family with a heterozygous β3 D723H variant as well as the first two families to be described outside of Japan with a heterozygous αIIb R995W substitution. Significantly, not only both of these variants of the αIIbR995/β3D723 salt bridge give rise to moderate MTP and platelet function defects; their platelets also contained enlarged α-granules.

CASE HISTORIES

We now report three families (A from Reunion island; B and C from France) with inherited MTP transmitted across 2 or 3 generations suggestive of autosomal dominant (AD) inheritance. The family pedigrees are shown in Fig. 1 and the three index cases (AII.1 an adult female, BI.1 and CI.1 adult males) identified. Other family members known to have MTP and significant subpopulations of enlarged platelets are also highlighted. All showed moderate to mild thrombocytopenia and often a higher proportion of immature platelets when analyzed with the Sysmex XE-5000 automat (Sysmex,Villepinte, France) (Table I). Increased mean platelet volumes were observed for BI.1, CI.1, and C1.2 (Table I) but values are not given when the large diameter of many of the platelets meant that they were not taken into account by the machine (particularly so for members of family A with MTP). Other blood cell lineages were usually present for affected family members and all routinely tested coagulation parameters were normal. As quantitated by the ISTH-BAT bleeding score, members of family A with MTP were the most affected (Table I). For example, AII.1 suffered from severe menorrhagia and severe post-partum bleeding requiring platelet and red blood cell transfusions after her second childbirth although two other children were born without problems (including a cesarean section). AII.1 also experienced occasional spontaneous bruising and episodes of iron-deficient anemia of unknown cause. An affected sister also has easy bruising and childbirth was under the cover of platelet transfusion. In family B the index case BI.1 suffered epistaxis but no bleeding has been reported for other family members. No bleeding was seen for the index case (CI.1) in family C despite major surgery following a bomb explosion while working as a war photographer. His daughter (CII.1) however experiences mild bleeding with frequent hematomas. Our study was performed in accordance with the declaration of Helsinki after written informed consent, and met with the approved protocol from INSERM (RBM-04-14).

METHODS

Platelet aggregation

Platelet aggregation was tested in citrated platelet-rich plasma (PRP) according to our standard protocols (21) and compared to PRP from healthy control donors without adjustment of the platelet count. The following agonists were used: 10µM adenosine diphosphate (ADP); 1mM arachidonic acid (AA); 1µM U46619, (all from Sigma Aldrich, L'isle d'Abeau, Chesnes, France); 20 µM thrombin receptor activating peptide (TRAP) (Polypeptide Group, Strasbourg, France); 1µg/mL collagen (COL) (Chronolog Corporation, Havertown, USA); 5 µM, epinephrine (Sigma), 1.5 mg/mL, and 0.6 mg/mL ristocetin (Helena Biosciences Europe, Elitech, Salon-en-Provence, France). Results were expressed as percentage maximal intensity.

Flow cytometric analysis (FCM)

Glycoprotein expression on unstimulated platelets was assessed using citrated PRP according to our standard protocols (12, 21). On occasion, platelet surface labelling for αIIb, β3, GPIbα and P-selectin was quantified using the PLT Gp/Receptors kit (Biocytex, Marseille, France) at room temperature before and after stimulation with 10µM ADP and 50µM TRAP using the Beckman Coulter Navios flow cytometer (Beckman Coulter, Villepinte, France). Platelets were identified by their light scatter characteristics and their positivity for a PC5 conjugated platelet-specific monoclonal antibody (MoAb) (CD41). An isotype antibody was used as negative control. To study platelet αIIbβ3 activation by flow cytometry, platelets were activated with either 10 µM ADP or 20 µM TRAP in the presence of FITC-conjugated PAC-1. A fluorescence threshold was set to analyze only those platelets that had bound FITC-PAC1. In brief, an antibody mixture consisting of 40 µl of each MoAb (PAC-1 and CD41) was diluted with 280 µl of PBS. Subsequently 5µl of PRP were mixed with 40µl of the antibody mixture and with 5 µl of either saline or platelet activator. After incubating for 15 min at room temperature in the

dark, 1ml of isotonic PBS buffer was added and samples were analyzed. Antibody binding was expressed either as the mean fluorescence intensity or as the percentage of platelets positive for antibody.

Transmission electron microscopy (EM)

PRP from blood taken into citrate or ACDA anticoagulant was diluted and fixed in PBS, pH 7.2, containing 1.25 %(v/v) glutaraldehyde for 1h as described (12). After centrifugation and two PBS washings, they were post-fixed in 150 mM cacodylate-HCl buffer, pH 7.4, containing 1% osmium tetroxide for 30 min at 4°C. After dehydration in graded alcohol, embedding in EPON was performed by polymerization at 60°C for 72 h. Ultrathin sections 70-80 nm thick were mounted on 200-mesh copper grids, contrasted with uranyl acetate and lead citrate and examined using a JEOL JEM1400 transmission electron microscope equipped with a Gatan Orius 600 camera and Digital Micrograph software (Lyon Bio Image, Centre d'Imagerie Quantitative de Lyon Est, France). Morphometric measurements were made using Image J software (National Institutes of Health, USA).

Genetic analysis and mutation screening.

DNA from AII.1, BI.1 and CI.1 was subjected to targeted exome sequencing (v5-70 Mb) as part of a study of a series of families with MTP due to unknown causes organized within the Paris Trousseau Children's Hospital (Paris, France). Single missense variants known to be pathological for MTP in the *ITGA2B* and *ITGB3* cytoplasmic tails were highlighted and their presence in other family members with MTP was confirmed by Sanger sequencing (primers are available on request). The absence of other potentially pathological variants in genes known to be causal of MTP in the targeted exome sequencing analysis was confirmed.

In silico models to investigate αIIbβ3 structural changes induced by the mutations were obtained using the PyMOL Molecular Graphics System, version 1.3, Schrödinger, LLC

(www.pymol.org) and 2k9j pdb files for transmembrane and cytosolic domains as described in our previous publications (3,4,12). Amino acid changes are visualized in the rotamer form showing side change orientations incorporated from the Dunbrack Backbone library with maximum probability.

In vitro MK differentiation, ploidy analyses, quantification of proplatelets and immunofluorescence analysis

Plasma thrombopoietin (TPO) levels were measured as previously described (21). Patient or control $CD34^+$ cells were isolated using an immunomagnetic beads technique (Miltenyi, Biotec, France) and grown supplemented with 10 ng/mL TPO (Kirin Brewery, Tokyo, Japan) and 25 ng/mL Stem Cell Factor (SCF; Biovitrum AB, Stockholm, Sweden).

(*i) Ploidy analyses.* At day 10, Hoechst 33342 dye (10 µg/mL; Sigma-Aldrich, Saint Quentin Fallavier, France) was added to the medium of cultured MKs for 2 h at 37°C. Cells were then stained with directly coupled MoAbs: anti–CD41-phycoerythrin and anti-CD42a-allophycocyanin (BD Biosciences, Le Pont de Claix, France) for 30 min at 4°C. Ploidy was measured in the $CD41^+CD42^+$ cell population by means of an Influx flow cytometer (BD; Mountain View,USA) and calculated as previously described (21).

*(ii) Quantification of proplatelet-bearing MKs***.** To evaluate the percentage of MKs forming proplatelets (PPTs) in liquid medium, $CD41^+$ cells were sorted at day 6 of culture and plated in 96-well plates at a concentration of 2000 cells per well in serum-free medium in the presence of TPO (10 ng/mL). MKs displaying PPTs were quantified between day 11 and 13 of culture by enumerating 200 cells per well using an inverted microscope (Carl Zeiss, Göttingen, Germany) at a magnification of ×200. MKs displaying PPTs were defined as cells exhibiting ≥1 cytoplasmic process with constriction areas and were analyzed in triplicate in two independent experiments for each individual.

(iii) Fluorescence microscopy. Primary MKs grown in serum-free medium were allowed to spread for 1 h at 37 °C on 100 μg/mL fibrinogen (Sigma Aldrich, Saint Quentin Fallavier, France) coated slides, then fixed in 4% paraformaldehyde (PFA), washed and permeabilized for 5 min with 0.2% Triton-X100 and washed with PBS prior to being incubated with rabbit anti-VWF antibody (Dako, Les Ulis, France) for 1 h, followed by incubation with Alexa 546-conjugated goat anti-rabbit immunoglobulin G (IgG) for 30 min and Phalloidin-FITC (Molecular Probes, Saint Aubin, France). Finally, slides were mounted using Vectashield with 4, 6 diamidino-2-phenylindole (Molecular Probes, Saint Aubin, France). The PPT-forming MKs (cells expressing VWF) were examined under a Leica DMI 4000, SPE laser scanning microscope (Leica Microsystems, France) with a 63×/1.4 numeric aperture oil objective.

RESULTS

Molecular genetic analysis:

We describe 3 previously unreported families, one based in Reunion Island and the others in France, with inherited MTP and mild to moderate bleeding. Targeted exome sequencing revealed heterozygous missense mutations of residues that compose the platelet αIIbR995/β3D723 intracytoplasmic salt bridge whose loss is integral to integrin signaling. Probands AII.1 and BI.1 have the αIIbR955W variant previously identified in Japanese families with MTP (9). In contrast CI.1 possesses β3D723H originally described as a nonsynonymous SNP and associated with MTP in a UK family (7). Sanger sequencing confirmed the presence of both variants and showed that their expression segregated with MTP in the family members available for genetic analysis (see Fig. 1 for families A, B and C) and absent from the subjects AIII.1, BI.2, CII.2 A who have a normal platelet count. The structural effect of the mutations was studied using the sculpting function incorporated in the PyMol in silico modeling program (see Methods); the images in Fig. 1 show the transmembrane and cytoplasmic domain segments of αIIb (blue) and β3 (green). The interactions creating the inner membrane association clasp are highlighted for wild type αIIbβ3 in dashed circles with the positive αIIbR995 and negative β3D723 represented as sticks. Both substitutions result in steric interference, especially when β3D723 is replaced by the larger H. The substitutions of αIIbR995 with neutral W or β3D723 with the positive H necessarily weaken or abrogate the salt bridge potentially leading to a separation of the subunit tails. Secondary influences also extend to other membrane proximal amino acids in π interactions shown as sticks and transparent spheres (see Discussion).

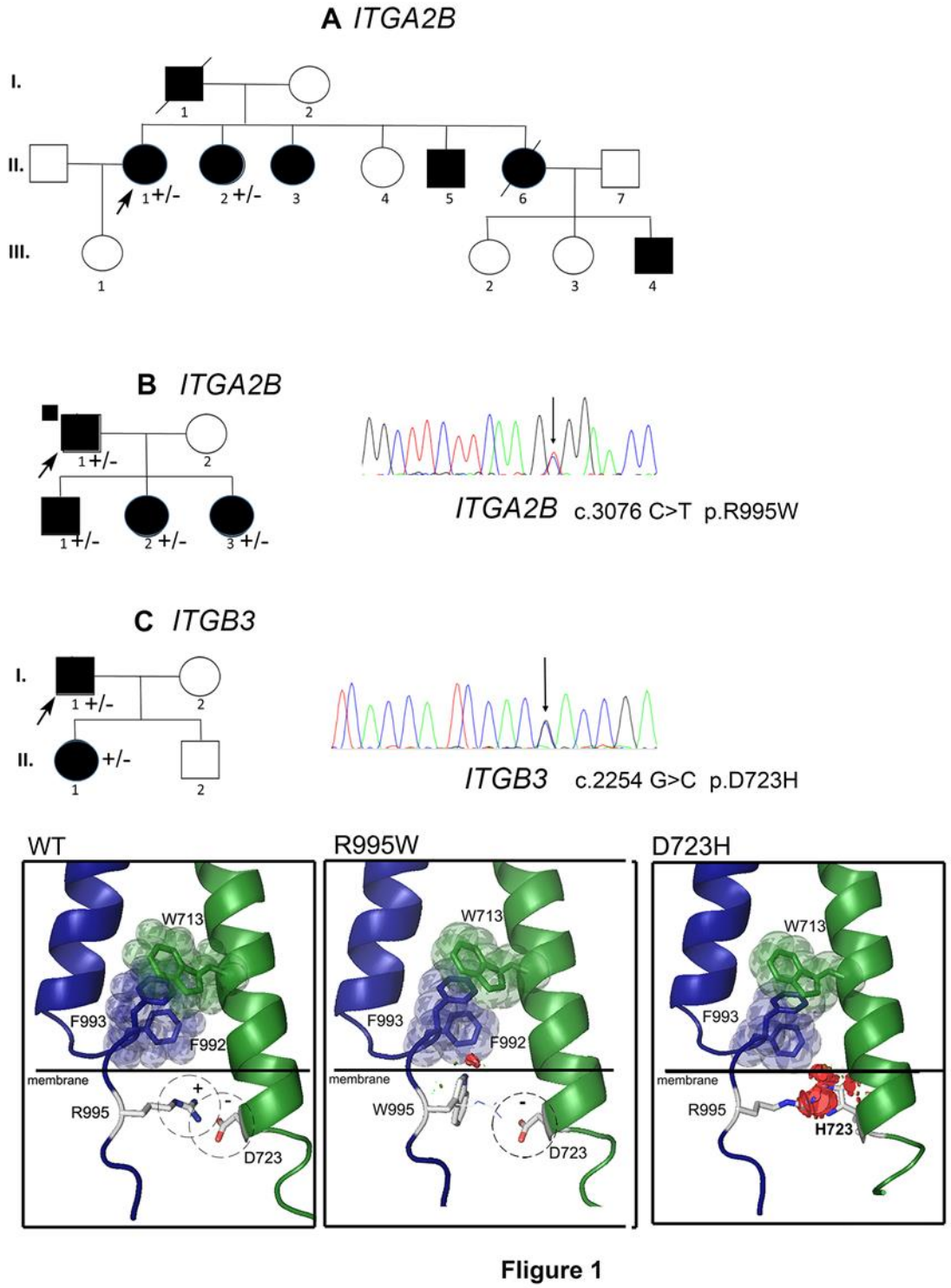

Fligure 1

Fig. 1. Genetic analysis and structural in silico modeling of the αIIb R995W and the β3 D723H mutations. First shown are the three family pedigrees (A-B-C). Dark symbols indicate MTP while non-filled symbols indicate a normal platelet count. Arrows identify the index cases for which heterozygous

ITGA2B R995W (A, B) and *ITGB3* D723H (C) variants were first highlighted by targeted exome sequencing. The coding regions of the *ITGA2B* and *ITGB3* genes were then amplified from genomic DNA of index cases and family members by polymerase chain reaction and amplified DNA fragments were subjected to direct cycle Sanger sequencing. As illustrated for AII.1 and BI.1, a C-to-T transition at nucleotide 3076 (3076C>T), changing R995 to W for *ITGA2B*, and for CI.1 a G-to-C transition at nucleotide 2254 (2254G>C) changing D723 to H for *ITGB3*, were detected. A vertical arrow shows the position of the substitution on the sequencing histograms. The penetrance of the mutation within each family is shown on each pedigree (+/-). In the lower panel, cartoons obtained through in silico PyMOL modeling show how αIIbR995W and β3D723H influence interactions between the transmembrane and cytoplasmic domains. The first relates to W713 of β3 and F992 and F993 of αIIb. This association motif consists of π interactions and aromatic cycle stacking. Two other well conserved motifs (GFFKR and HDR(R/K)E for αIIb and β3, respectively) localize close to the cytoplasmic face of the membrane with the formation of a salt bridge involving the positively charged R995 of αIIb and the negatively charged D723 of β3 (25). In the cartoon, αIIb is in blue while β3 is in green; aromatic amino acids involved in π interactions are shown as sticks and transparent spheres. The salt bridge is represented as dashed circles, with the positive αIIb-R995 and the negative β3-D723 as sticks. The graphical "bumps" (red discs) reveal steric encumbrance caused by the amino acid substitution. The D723H mutation (family C) results in the replacement of the negatively charged D by the positively charged and larger H. The overall potential effect of repulsive charges and steric encumbrance promote separation of the two transmembrane segments. Similar but less extensive changes are seen when Arg995 is substituted with the neutral W.

Platelet aggregation and flow cytometry analysis:

Citrated PRP from each index case was stimulated with ADP, TRAP, AA and collagen and platelet aggregation measured using standard procedures (Fig. 2A). Results were variable, and taking the curves obtained for ristocetin as a control of the low platelet count for each index case platelets from each family with αIIbR995 and β3D723 variants retained at least a partial aggregation response with family AII.1 showing the largest loss – particularly for TRAP. The response to epinephrine was also much reduced or absent for all samples (data not illustrated). Striking was the low response to AA for patients CI.1and CII.2, a finding reversed on addition

of the thromboxane A2 analog U46619 (data not shown). Otherwise, the platelets retained a rapid response to ADP and collagen. Flow cytometry and MoAbs recognizing determinants specific for αIIb, β3 or the αIIbβ3 complex (data not shown) gave comparable results for each index case with surface levels for the 3 index cases ranging from 48 to 75% of those on normal platelets (Fig. 2B). Taking into account the increased platelet size, such intermediate levels would suggest that both mutations have a direct influence on αIIbβ3 expression. Enigmatically, the platelet expression of GPIb was particularly increased for the 4 tested family members (AII.1, AII.2, BI.1, BII.2) with the αIIbR995W mutation a finding only partially explained by the increased platelet volume of these patients with MTP. Binding of PAC-1 recognizing an activation-dependent epitope on αIIbβ3 was analyzed as a probe of the activation state of the integrin. Spontaneous binding of PAC-1 was seen for the platelets of index case AII.1 with the αIIbR995W mutation suggesting signs of activation but was not seen for the index case of the second family with this mutation or for the index case of the family with β3D723H (Fig. 2C). Studies were extended to platelets stimulated with high doses of ADP and TRAP; increased binding was seen for AII.1 consistent with further activation of the residual surface αIIbβ3 of the platelets. However, no binding was seen for BI.1 or C.I.1. suggesting that for these patients the residual αIIbβ3 was refractory to stimulation under the non-stirred conditions of this set of experiments (Fig. 2B).

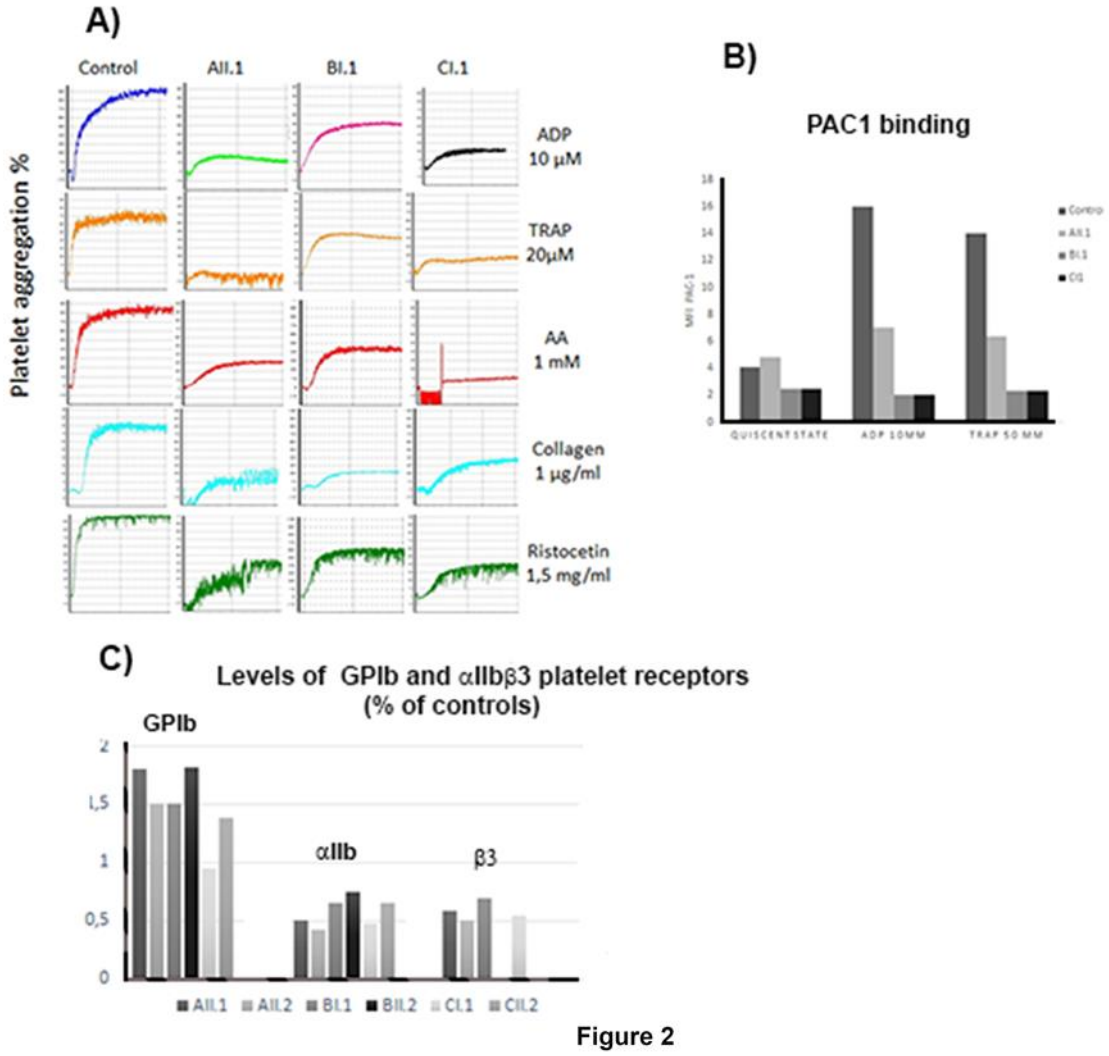

Fig. 2. Selected biological platelet findings for the three index cases. In A) Light transmission aggregometry performed in citrated platelet-rich plasma (PRP) compares typical responses of platelets from the index cases (AII.1, BI.1, CI.1) to that of a typical control donor. For AII.1 aggregation with high doses of ADP, Col, TRAP and AA were reduced compared to ristocetin-induced platelet agglutination whose intensity reflected the low platelet count of the patient. For BI.1 platelet aggregation was moderately reduced with Col and TRAP while for CI.1 platelet aggregation was reduced essentially for TRAP and AA (it should be noted that it was restored with the thromboxane receptor agonist U46619, not shown). In B) Spontaneous PAC1 binding evaluated by flow cytometry on resting platelets was marginally increased for AII.1 but not for the other index cases. Binding increased for AII.1 after platelet activation with ADP and TRAP but remained low compared to the control. In contrast, PAC-1 binding was basal for BI.1 and CI.1 even after addition of ADP or TRAP. In C) we illustrate the levels of GPIb and αIIbβ3 receptors evaluated by flow cytometry not only for the probands but also for other

selected family members. A decreased surface expression of αIIb and β3were found for all affected patients, values ranging between 43% (AII.2) and 70% (BII.2) of the control mean. Interestingly, levels of GPIb were increased for the patients and particularly so for families A and B with sometimes values beyond 150% of normal values.

Electron microscopy:

Platelets from the index cases of all 3 families were examined by transmission EM and for each subject a significant subpopulation of the platelets were larger than normal (Fig 3). Overall, the platelets showed wide size variations; many tended to be round in contrast to the discoid shape of controls (control platelets are illustrated by us in ref 12). Patients from all index cases possessed platelets with large variations in the numbers of vacuoles. Striking was a heterogeneous distribution of α-granules with the presence of giant forms particularly evident for patient AII.1 and what appears to represent granule fusion was seen (highlighted in panel 3b). All of the morphological changes were analyzed quantitatively; statistical significance was achieved for all measurements except for those concerning α-granule numbers of patient CI.1 with the β3D723H substitution (Fig. 3). Please note that the platelets of the patients with the αIIbR995W mutation tended to be larger and show more ultrastructural changes. Interestingly, the greater the frequency of giant granules, the lower is their concentration/μm^2. The presence of giant α-granules repeats what we have recently seen for a patient with a heterozygous β3718del and is reminiscent of the feature that we have much earlier described in Paris Trousseau syndrome (12, 22, and 23). Targeted exome sequencing failed to show mutations in the *FlI1* gene of the three index cases.

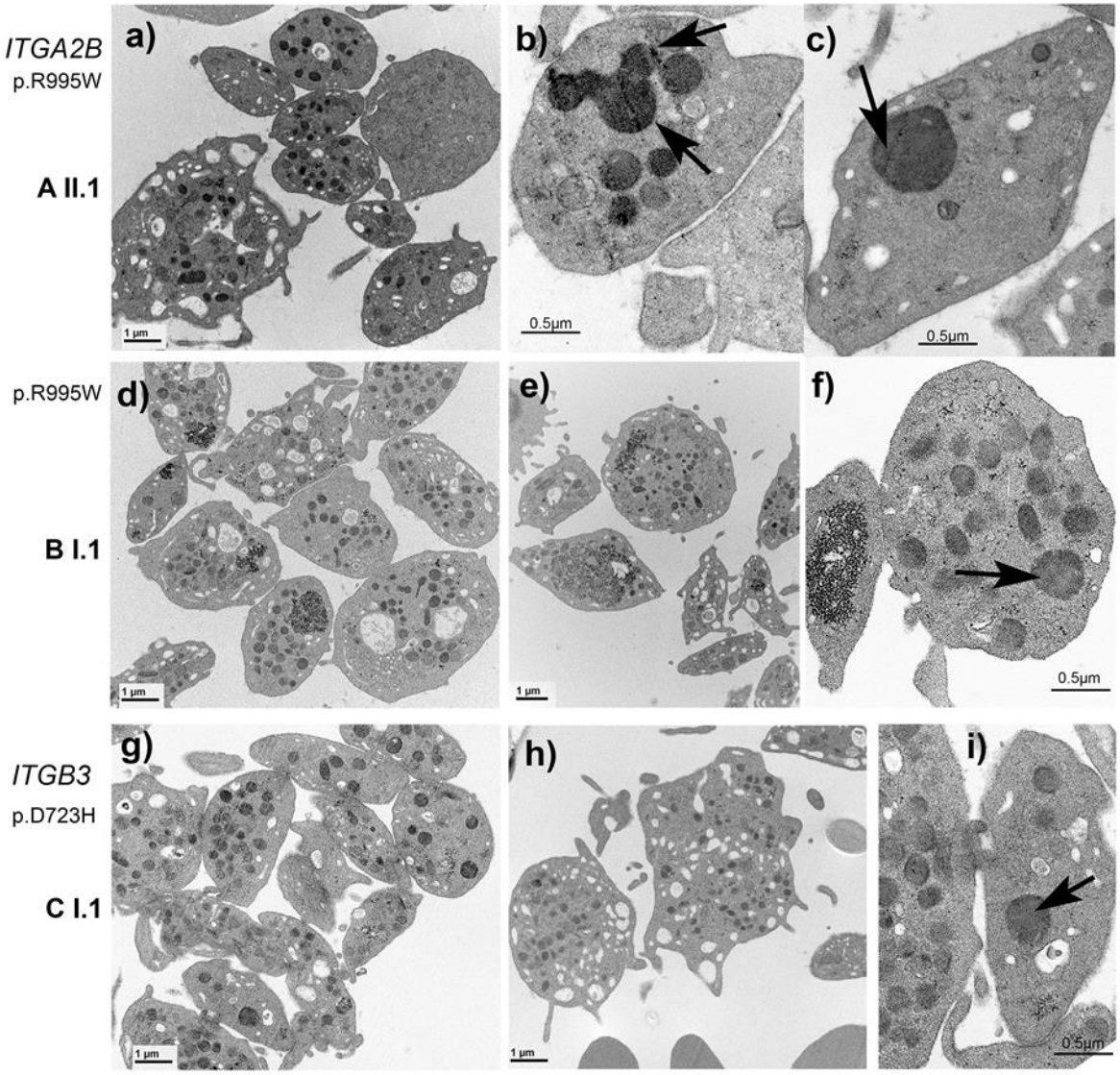

Groups (n)	Area [µm2]	Maximal diam [µm]	Minimal diam [µm]	Ratio Max/Min	Number α- granules per µm2	Diam α-granules [nm]	% α-granules >294nm diam
Control (825)	3.07±1.48	2.86±0.59	1.35±0.51	2.41±1.05	2.60±1.39	241±53	13
A II.1 (100)	6.10±4.20†	3.19±0.88†	2.24±0.86†	1.51±0.40†	1.38±0.92†	339±193†	47
B I.1(120)	5.77±3.65†	3.37±0.88†	2.04±0.81†	1.83±0.71†	2.28±2.08†	293±62†	43
C I.1 (100)	4.69±3.10†	3.19±0.85†	1.77±0.73†	2.03±0.81†	2.35±1.26	254±52	16

Figure 3

Fig. 3. Transmission electron microscopy of platelets from the index cases of each family with the corresponding quantitative morphometric analysis. Upper panels (a-c) show selected images obtained for AII.1 with the *ITGA2B* (R995W) mutation. Shown are enlarged platelets, with heterogeneity in granule distribution and the presence of occasional giant α-granules (b, c) sometimes appearing to show fusion

(see arrows in b) Middle panels (d, e, f) illustrate results for BI.1, index case of the second family with the same mutation *ITGA2B* (R995W). Here again, large round platelets (d-f) but also discoid platelets of normal size are present. An arrow highlights an enlarged α-granule in (f). The lower panels show images for CI.1 (g, h, i) with the *ITGB3* D723H mutation. Typical morphology of the platelets is shown with in (g) a group of platelets not so enlarged as those often seen for members of families A and B with MTP (an observation confirmed by the morphometric analysis). In (h) note two large platelets with the one on the right possibly representing an unfragmented part of MK cytoplasm. Occasional enlarged α -granules (arrow) are present as illustrated in (i); however, values for frequency and their size did not reach statistical significance (see morphometric analysis). Bars indicate the magnification of the illustrated EMs. Morphometric analyses of parameters relating to platelet size, shape and α-granule number and size are presented at the bottom of the Figure. Data are presented as mean ± SD. Statistical significance was determined by Student's t test for continuous variables. A p value<0.01 was considered as statistically significant (†) (n) corresponds to the number of platelet sections analysed.

Megakaryopoiesis:

Plasma TPO levels were within normal range for each of the index cases (Table I)**.** Analysis of MK maturation and development did not reveal any defect in early megakaryocyte maturation. Ploidy measured in the$CD41^+CD42^+$ cell population at day 10 of culture by means of an Influx flow cytometer with the proportion of 2N-32N MKs being within the normal range (Fig. 4). Proplatelet formation was examined on days 11 and 12 of culture using an inverted microscope and no difference in percentage of proplatelet bearing MKs was detected. Proplatelet morphology was analyzed at the same time using a SPE laser scanning microscope after dual fluorescent labeling of PFA-permeabilized cells with Phalloidin and antibody to VWF (green) (Fig. 4). While the mature MKs basically showed normal morphology proplatelet numbers tended to be lower and some extensions appeared swollen and with decreased branching. Another finding was that the size of the tips and bulges occurring at intervals along the proplatelets tended to be larger than for control MKs and especially so for the two index cases with αIIbR995W (AII.1 and BI.1); an image of a giant granule can be observed in an illustrated extension of AII.1 (Fig 4, yellow arrow).

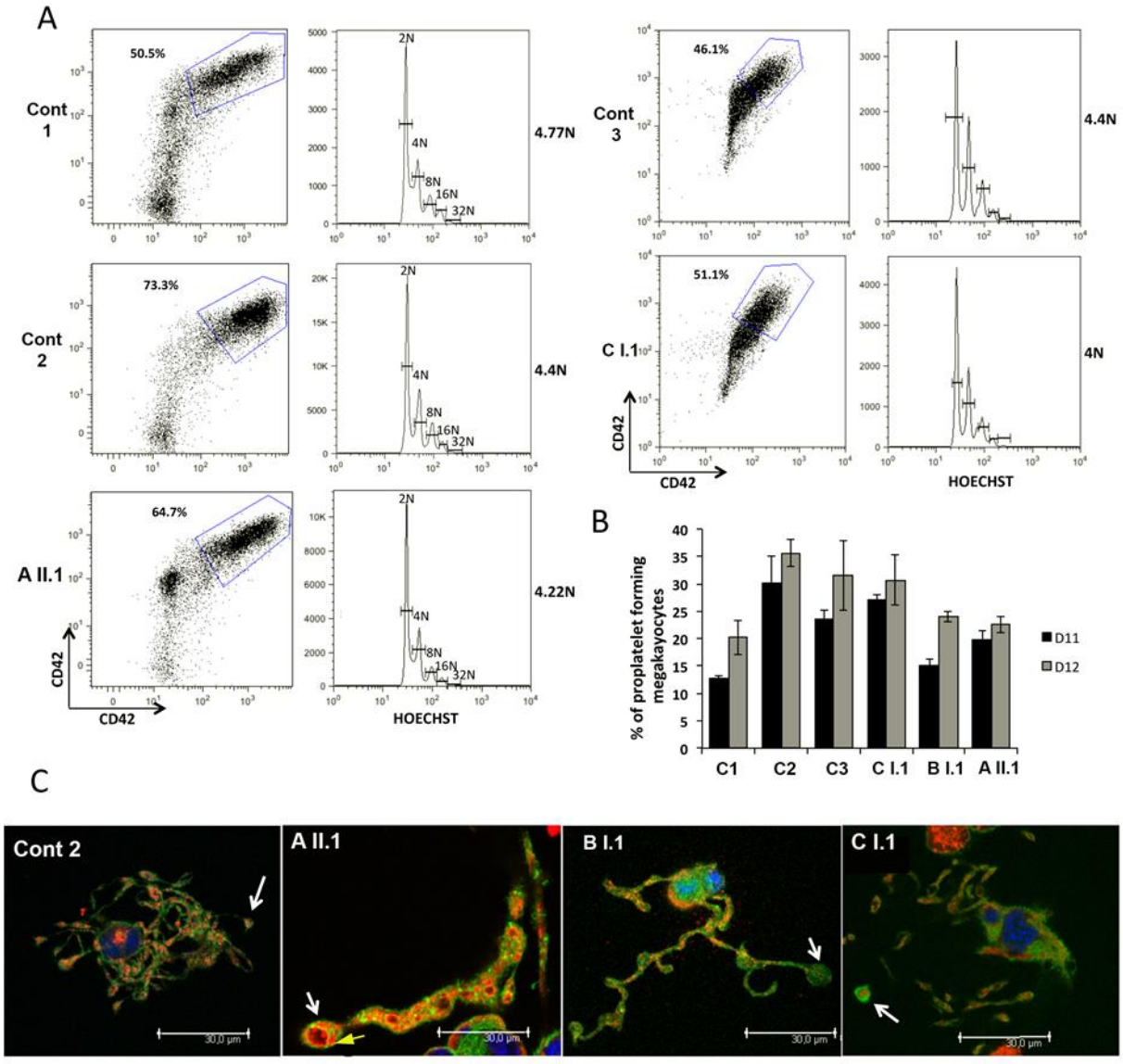

Figure 4

Fig. 4. In vitro derived MK differentiation. MK differentiation was induced from control (Cont1, Cont2) or patient (AII.1, BI.1 and CI.1) peripheral blood $CD34^+$ cells. (A) Gates represent mature ($CD41^+CD42^+$) MKs (left panel). The ploidy level (N) was analyzed in the gate of $CD41^+CD42^+$ MKs and was based on the percentage of cells in 2N, 4N, 8N, 16N and 32N gates. (B) The percentage of PPT forming MKs was estimated by counting MKs exhibiting one or more cytoplasmic processes with areas of constriction at day 11 and 12 of culture. A total of 200 cells per well was counted. The histograms show one of two independent experiments with similar results. Each experiment was performed in triplicate and the error bars represent mean ±SD. **(**C) Immunoconfocal analysis of platelet-like structures and proplatelets generated from control or patient MKs. Proplatelet forming MKs were plated on fibrinogen at day 13 of culture and stained with phalloidin (green) and rabbit anti-VWF (red)

antibody. The nucleus was stained with DAPI (bleu). Confocal imaging was performed on a Leica TCS SP8 inverted laser scanning confocal microscope. All images were acquired using an oil immersion 63x objective (1,4 NA). White arrows indicate the proplatelet tips with increased size. Yellow arrow indicate a VWF-labelled granule with enlarged size.

DISCUSSION

In the resting state, the trans-membrane and intra-cytoplasmic segments of the two subunits of αIIbβ3 interact, an interaction that is key to maintaining the extracellular domain of the integrin in its bent resting state (15, 25). One area of contact between the cytoplasmic tails involves π interactions and aromatic cycle stacking of consecutive F residues within the highly conserved αIIb GFFKR (aa991-955) sequence with W713 of β3 (shown in Fig. 1). A second interaction principally involves a salt bridge between the positively charged αIIbR995 and negatively charged β3D723 (13-15). Early studies including site-directed mutagenesis, truncation models and charge reversal mutations showed that loss of this intra-molecular clasp led to integrin activation and modified function (13, 14). Hence the mutations described in our patients are of high significance for integrin biology. Enigmatically, the β3D723H change has the more pronounced structural effect resulting in (i) repulsive electrical charge forces with the positively charged H now facing the positively charged R995 and (ii) steric encumbrance due to the larger H. The net result is a widening of the interval between R995 and H723 and a weakening of the salt bridge, changes that accompany the acquisition of a higher affinity state (26). Of similar consequence but milder in nature is the replacement of αIIb995R by the neutral W while both mutations potentially also interfere with π interactions involving αIIbF992.

A novel feature of our study is the presence of enlarged α-granules in the platelets of all 3 index cases. This is of interest for we have recently reported enlarged α-granules for a patient with MTP associated with a β3 L718del resulting in loss of synchronization between opposing amino acids of the αIIb and β3 cytoplasmic tails and a weakening of the αIIbR995/β3D723 salt bridge (Table SI) (12). The presence of enlarged α-granules in platelets of patients from 3 unrelated families with MTP linked to cytoplasmic tail mutations in *ITGA2B* or *ITGB3* in our current study strongly suggests that they have a role in the ultrastructural changes with emphasis on the αIIbR995W mutation. But further studies will be required to define this role and rule out

secondary genetic variants in linkage disequilibrium with the primary mutations. Classically, enlarged α-granules are a consistent feature of the Paris-Trousseau syndrome first being seen on stained blood smears and then confirmed by EM (22,23). Paris-Trousseau syndrome results from genetic variants and haplodeficiency of the *FLI1* transcription factor (27), variants that were absent from our families when studied by targeted exome sequencing. For our previously studied patient with the L718del, immunogold labeling and EM clearly showed the association of P-selectin, αIIbβ3 and fibrinogen with the giant α-granules suggesting a normal initial granule biosynthesis (12). Whether the giant granules are formed as part of the secretory pathway, as has been proposed for normal platelets (28), or perhaps are the consequences of premature apoptosis remain subjects for further study. In this context it would be interesting to know if they are more abundant in aging platelets and at what stage they appear in maturing MK and/or during platelet biogenesis. Preliminary immunofluorescence studies showed what appeared to giant granules in the proplatelets of cultured megakaryocytes from AII.1. It is also important to know if enlarged α-granules have been overlooked in previously published cases of cytoplasmic tail mutations affecting αIIbβ3 or are restricted to certain cases. In parallel, we also keep in mind that FLI-1 with others transcription factors coregulate directly *ITGA2B* and *ITGB3* (24).

The genotypes and phenotypes of previously published cases associating cytoplasmic tail mutations of αIIb or β3 and MTP are compared in Table S1. There is much phenotypic variability but as in our cases all give rise to a mild to moderate thrombocytopenia and platelet size variations including giant forms. Inheritance is AD when family studies permit this conclusion, although two reports associate single allele missense mutations of the αIIb cytoplasmic tail with a second and different mutation causing loss of expression of the second allele (6,10). Such a loss may exaggerate the effect of single allele missense mutations in these cases. In all but one of the published cases bleeding was mild to moderate or was absent and

our cases follow this pattern. Platelet aggregation was never totally abrogated but tended to occur more slowly with a reduced final intensity as was largely the case for families A and B in our study. Platelets of family C (β3D723H) retained a good aggregation response, a finding in agreement with the report on the UK family with the same mutation (7). For families A, B and C intermediate levels of αIIbβ3 were shown at the surface, results again consistent with many of the literature reports (Table S1). It is noteworthy that the platelet aggregation response of obligate heterozygotes for classic type I GT is normal (2) suggesting that despite the influence of the low platelet count, the cytoplasmic domain mutations have a direct effect on the platelet aggregation response. Interestingly, a low platelet surface αIIbβ3 expression was shown to be associated with normal internal pools of αIIbβ3 in patients with αIIbR995Q and αIIbR99W substitutions suggesting defects in integrin recycling (5,10). Our results for family C with intermediate platelet surface levels of αIIbβ3 differed from the results for the UK family where αIIbβ3 expression was normal (7). Expression of the adhesion receptor GPIb was increased on the platelets of our index cases and especially so for the two with the αIIbR995W variant a finding that was previously observed for Japanese cases with the same mutation (9). The reason for this is not known but could reflect altered megakaryopoiesis.

A feature of cytoplasmic domain mutations causal of MTP is that long-range conformational changes extend to the functional domains of the integrin and give what is often termed a partially activated state (6-12) (Table S1). This was indeed shown by Hughes et al (13,14) who expressed αIIbβ3 in CHO cells after modifying residues of the salt bridge through site-directed mutagenesis. While the changes permit binding of the activation-dependent IgM MoAb PAC-1, only for one report has spontaneous binding of Fg been observed for this class of mutation (11). These results therefore differ from the C560R mutation in the β3 cysteine-rich β (A) extracellular domain as reported for a French patient whose platelets circulated with αIIbβ3-bound Fg (29). The conformational changes permitting spontaneous PAC-1 binding but

only rarely Fg binding remain to be defined although αIIbβ3 clustering remains a potential explanation (8). The activation state of αIIbβ3 is also often greater in transfected heterologous cells than for platelets of the patients themselves perhaps due to abnormal recycling and concentration of the mutated integrin in internal pools. Unexpectedly, variable or no PAC-1 binding in our patients was seen after stimulation with TRAP despite these patients showing a residual aggregation response in citrated PRP. This apparent contradiction is possible related to the non-stirred conditions of the in vitro PAC-1 binding experiments. As patients from family C showed a markedly abnormal response to AA, a role for thromboxane A2 generation in αIIbβ3 activation merits investigation.

Previous studies have examined MK maturation in culture but have largely been performed for patients with a 40 amino acid del (p.647-686) in the β3 extracellular β-tail domain causal of MTP (17- 19). Among the changes that were noted were (i) fewer proplatelets and (ii) tips of larger size; changes associated with abnormal MK spreading on Fg and a disordered actin distribution and cytoskeletal defects seemingly linked to a sustained "outside-in" signaling induced by the constitutively active αIIbβ3 (17-19). Analysis of megakaryopoiesis for our patients did not reveal a defect in MK maturation or in ploidy but confirmed the above studies and previous studies on MKs from Japanese families with αIIbR995W (9) or the UK family with β3D723H defect in that abnormal proplatelet formation with decreased branching and with bulges of increased size at their tips. This defect was quite similar between our patients even if the size of tips seemed larger for the patients with αIIbR995W. The relationship between defects in αIIbβ3 complexes to changes in α-granule size remains to be determined. VWF-labelled granules with increased size were detected already in proplatelets in AII.1 and interestingly for the three patients studied, the larger the platelet surface area the larger the α-granule diameter suggesting that the defect responsible for increased platelet size contributes also to determination of α-granule size. The cause of the apparent fusion or coalescing of granules as

a mechanism of forming the giant granules not only observed for this patient but also for the β3 Leu718 deletion (12) merits further study. The fact that mutations modifying the salt bridge between the positively charged αIIbR995 and negatively charged β3D723 is particularly intriguing.

Our results therefore support a generalized hypothesis where mutations within αIIb or β3 cytoplasmic domains somehow lead to a facilitated MK surface interaction with stromal proteins in the marrow medullary compartment that in turn promote cytoskeletal changes that not only lead to altered proplatelet formation and platelet biogenesis but also, at least on occasion, an altered α-granule maturation.

Footnote

* Human Genome Variation Society nomenclature for the αIIb and β3 mature proteins are used in this study.

Acknowledgment: the authors thank N.Saut for her technical expertise for sequencing.

REFERENCES

1. Coller BS, Shattil SA. The GPIIb/IIIa (integrin αIIbβ3) odyssey: a technology-driven saga of a receptor with twists, turns, and even a bend. Blood 2008; 112(8):3011-3025.
2. George JN, Caen JP, Nurden AT. Glanzmann's thrombasthenia: The spectrum of clinical disease. Blood 1990; 75:1383-1395.
3. Nurden AT, Fiore M, Nurden P, Pillois X. Glanzmann thrombasthenia: a review of ITGA2B and ITGB3 defects with emphasis on variants, phenotypic variability, and mouse models. Blood 2011; 118:5996-6005.
4. Nurden AT, Pillois X, Fiore M, Heilig R, Nurden AT. Glanzmann thrombasthenia-like syndromes associated with macrothrombocytopenias and mutations in the genes encoding the αIIbβ3 integrin. Semin Thromb Hemost 2011; 37:698-706.
5. Hardisty R, Pidard D, Cox A, Nokes T, Legrand C, Bouillot C, Pannocchia A, Heilmann E, Hourdillé P, Bellucci S, Nurden AT. A defect of platelet aggregation associated with an abnormal distribution of glycoprotein IIb-IIIa complexes within the platelet: The cause of a lifelong bleeding disorder. Blood 1992; 80:696-708.
6. Peyruchaud O, Nurden AT, Milet S, Macchi L, Pannochia A, Bray PF, Kieffer N, Bourre F. R to Q amino acid substitution in the GFFKR sequence of the cytoplasmic domain of the integrin αIIb subunit in a patient with a Glanzmann's thrombasthenia-like syndrome. Blood 1998; 92:4178-4187.
7. Ghevaert C, Salsmann A, Watkins NA, Schaffner-Reckinger E, Rankin A, Garner SF, Stephens J, Smith GA, Debili N, Vainchenker W, de Groot PG, Huntington JA, Laffan M, Kieffer N, Ouwehand WH. A nonsynonymous SNP in the ITGB3 gene disrupts the conserved membrane-proximal cytoplasmic salt bridge in the αIIbβ3 integrin and cosegregates dominantly with abnormal proplatelet formation and macrothrombocytopenia. Blood 2008; 111:3407-3414.

8. Jayo A, Conde I, Lastres P, Martinez C, Rivera J, Vivcente V, Gonzalez-Manchon C. L718P mutation in the membrane-proximal cytoplasmic tail of β3 promotes abnormal αIIbβ3 clustering and lipid microdomain coalesce, and associates with a thrombasthenia-like phenotype. Haematologica 2010; 95:1158-1166.
9. Kunishima S, Kashiwagi H, Otsu M, Takayama N, Eto K, Onodera M, Miyajima Y, Takamatsu Y, Suzumiya J, Matsubara K, Tomiyama Y, Saito H. Heterozygous ITGA2B R995W mutation inducing constitutive activation of the αIIbβ3 receptor affects proplatelet formation and causes congenital macrothrombocytopenia. Blood. 2011; 117:5479-5484.
10. Kashiwagi H, Kunishima S, Kiyomizu K, Amano Y, Shimada H, Morishita M, Kanakura Y, Tomiyama Y. Demonstration of novel gain-of-function mutations of αIIbβ3: association with macrothrombocytopenia and Glanzmann thrombasthenia-like phenotype. Mol Genet Genomic Med 2013; 1:77-86.
11. Kobayashi Y, Matsui H, Kanai A, Tsumura M, Okada S, Miki M, Nakamura K, Kunishima S, Inaba T, Kobayashi M. Identification of the integrin β3 L718P mutation in a pedigree with autosomal dominant thrombocytopenia with anisocytosis. Br J Haematol 2013; 160:521-529.
12. Nurden P, Bordet J-C, Pillois X, Nurden AT. An intracytoplasmic β3 Leu718 deletion in a patient with a novel platelet phenotype. Blood Adv 2017; 1:494-499.
13. Hughes PE, O'Toole TE, Vlanne J, Shattil SJ, Ginsberg MH. The conserved membrane-proximal region of an integrin cytoplasmic domain specifies ligand-binding affinity. J Biol Chem 1995; 270:12411-12417.
14. Hughes PE, Diaz-Gonzalez F, Leong L, Wu C, McDonald JA, Shattil SJ, Ginsberg MH. Breaking the integrin hinge. A defined structural constraint regulates integrin signaling. J Biol Chem 1996; 271:6571-6574.

15. Kim C, Lau TL, Ulmer TS, Ginsberg MH. Interactions of platelet integrin αIIb and β3 transmembrane domains in mammalian cell membranes and their role in integrin activation. Blood 2009; 113:4747-4753.
16. Shattil SJ, Hoxie JA, Cunningham M, Brass LF. Changes in the platelet membrane glycoprotein IIb.IIIa complex during platelet activation. J Biol Chem 1985; 260:11107-11114.
17. Bury L, Malara A, Gresele P, Balduini A. Outside-in signaling generated by a constitutively activated integrin αIIbβ3 impairs proplatelet formation in human megakaryocytes. PLoS ONE 2012; 7:e34449. Doi:10.1371/journal.pone.0034449.
18. Bury L, Falcinelli E, Chiasserini D, Springer TA, Italiano Jr JE, Gresele P. Cytoskeletal perturbation leads to platelet dysfunction and thrombocytopenia in variant forms of Glanzmann thrombasthenia. Haematologica 2016; 101:46-56.
19. Hauschner H, Mor-Cohen R, Messineo S, Mansour W, Seligsohn U, Savoia A, Rosenberg N. Abnormal cytoplasmic extensions associated with active αIIbβ3 are probably the cause for macrothrombocytopenia in Glanzmann thrombasthenia-like syndrome. Blood Coagul Fibrinolysis 2015; 26:302-308.
20. Wang R, Shattil SJ, Ambruso DR, Newman PJ. Truncation of the cytoplasmic domain of beta3 in a variant form of Glanzmann thrombasthenia abrogates signaling through the integrin alphaIIbbeta3 complex. J Clin Invest. 1997; 100:2393-2403.
21. Bluteau D, Balduini A, Balayn N, Currao N, Nurden P, Deswarte C, Leverger G, Norris P, Perotta S, Solary E, Vainchencker W, Debili N, Favier R, Raslova H. Thrombocytopenia-associated mutations in the ANKRD26 gene regulatory region induce MAPK hyperactivation. JCI 2014; 124:584-591.

22. Breton-Gorius J, Favier R, Guichard J, Cherif D, Berger R, Debili N, Wainchenker W, Douay L. A new congenital dysmegakaryopoietic thrombocytopenia (Paris-Trousseau) associated with giant platelet α-granules and chromosome 11 deletion at 11q23. Blood 1995; 85:1806-1814.
23. Favier R, Jondeau K, Boutard P, Grossfeld P, Reinert P, Jones C, Bertoni F, Cramer EM. Paris-Trousseau syndrome: clinical, hematological, molecular data of ten cases. Thromb Haemost 2003; 90:893-897.
24. Tijssen MR, Cvejic A, Joshi A, Hannah RL, Ferreira R, Forrai A, Bellissimo DC, Oram SH, Smethurst PA, Wilson NK, Wang X, Ottersbach K, Stemple DL, Green AR, Ouwehand WH, Göttgens B. Genome-wide analysis of simultaneous GATA1/2, RUNX1, FLI1, and SCL binding in megakaryocytes identifies hematopoietic regulators. Dev Cell 2011; 20:597-609.
25. Litinov RI, Vilaire G, Li W, DeGrado WF, Weisel JW, Bennett JS. Activation of individual alphaIIbbeta3 integrin molecules by disruption of transmembrane domain interactions in the absence of clustering. Biochemistry 2006; 45:4957-4964.
26. Adair BD, Yeager M. Three-dimensional model of the human platelet integrin alphaIIbbeta3 based on electron cryomicroscopy and x-ray crystallography. Proc Natl Acad Sci 2002; 99:14059-14064.
27. Favier R, Raslova H. Progress in understanding the diagnosis and molecular genetics of macrothrombocytopenia. Br J Haematol 2015; 170:626-639.
28. Eckly A, Rinckel JY, Proamer F, Ulas N, Joshi S, Whiteheart SW, Gachet C. Respective contributions of single and compound granule fusion to secretion by activated platelets. Blood 2016; 128:2538-2549.

29. Ruiz C, Liu CY, Sun QH, Sigaud-Fiks M, Fressinaud E, Muller JY, Nurden P, Nurden AT, Newman PJ, Valentin N. A point mutation in the cysteine-rich domain of glycoprotein (GP) IIIa results in the expression of a GPIIb-IIIa (alphaIIbbeta3) integrin receptor locked in a high-affinity state and a Glanzmann thrombasthenia-like phenotype. Blood 2001; 98:2432-2441.